

## Technical and economical feasibility of using GGBS in long-span concrete structures

Kangkang Tang<sup>\*1</sup>, Steve Millard<sup>2a</sup> and Greg Beattie<sup>3b</sup>

<sup>1</sup>Department of Civil Engineering, Xi'an Jiaotong-Liverpool University, China

<sup>2</sup>Department of Engineering, University of Liverpool, UK

<sup>3</sup>Arup, UK

(Received August 27, 2014, Revised November 20, 2014, Accepted November 30, 2014)

**Abstract.** China accounts for nearly half of the global steel production. As a waste material or a by-product in the manufacture process, a large amount of blast furnace slag is generated every year. The majority of recycled blast furnace slag is used as an additive in low-grade blended cement in China (equivalent to the UK CEM II or CEM III depending on the slag content). The cost of using ground granulated blast furnace slag (GGBS) in such low-grade applications may not be entirely reimbursed based on market research. This paper reports an on-going project at Xi'an Jiaotong-Liverpool University (XJTLU) which investigates the feasibility of using GGBS in long-span concrete structures by avoiding/reducing the use of crack control reinforcement. Based on a case study investigation, with up to 50% of CEM I cement replaced with GGBS, a beneficiary effect of reduced thermal contraction is achieved in long-span concrete slabs with no significant detrimental effect on early-age strengths. It is believed that this finding may be transferable from China to other Asian countries with similar climates and economic/environmental concerns.

**Keywords:** concrete thermal contraction; finite element analysis

---

### 1. Introduction

China accounts for nearly 50% of the global steel production and over 80 million tonnes of blast furnace slag is generated annually (Tang 2014). GB/T 18046-2008 (2008), the Chinese standard for GGBS used in concrete, recognises that blast furnace slag, ground to an appropriate fineness, can be used in concrete. The majority of recycled blast furnace slag is however used as an additive in low grade blended cement in China and the cost may not be entirely reimbursed (Tang *et al.* 2013). Fluctuations in ambient temperature due to changing environmental conditions will cause structural concrete to expand or contract. Linear expansion and subsequent contraction will also take place in concrete at an early age due to the exothermic cement hydration reaction and autogenous shrinkage. Significant internal stresses will build up in long-span concrete beams or slabs if these movements are externally restrained by supporting columns or shear walls. The

---

\*Corresponding author, Lecturer (PhD, CEng, MICE), E-mail: [Kangkangtang@gmail.com](mailto:Kangkangtang@gmail.com)

<sup>a</sup>Emeritus Professor

<sup>b</sup>Associate Director

magnitude of the induced tensile stresses therefore must be calculated to ensure that the crack widths are less than the maximum acceptable size. A maximum crack width in reinforced concrete sections is therefore required at the Serviceability Limit State (SLS) by Eurocode 2 (2004) and GB 50010-2002 (2002). One of the typical procedures adopted in China to minimise early-age tensile cracking is to leave one-metre wide gaps in slabs and beams when concrete is poured (Fig. 1). These gaps will not be filled until early-age concrete hydration contraction has been completed on both sides. There are however some drawbacks associated with this provision. Additional structural supports along both edges of the movement joint are required to enable independent stability on each side. As an alternative solution, it is an effective engineering practice to limit concrete crack widths by using supplementary crack control reinforcement which however will increase the overall cost.

It is important to determine the heat development during cement hydration, especially for large volume concrete pours. The semi-adiabatic calorimetry test is a common method used to investigate and predict hydration temperatures in mass concrete. Concrete specimens are cured semi-adiabatically to simulate the curing conditions of mass concrete (Azenha *et al.* 2009, Kim *et al.* 2011 and Lawrence *et al.* 2012). Da Silva *et al.* (2013) successfully predicted the hydration temperature development in a 1050m<sup>3</sup> concrete foundation based on the experimental results obtained from a 1 m<sup>3</sup> concrete cube specimen cured under the semi-adiabatic curing condition. The heat development during early-age setting and curing in concrete mixes containing GGBS as a partial cement replacement is slower than that of the ordinary CEM I mixes. This was attributed to a two-stage hydration process of GGBS, i.e. GGBS first reacts with alkali hydroxide and then with calcium hydroxide released by the hydrated cement (Regourd 1983). The low early-age strength development in GGBS concrete could also be attributed to this two-stage effect. A higher curing temperature however will increase the amount of alkali hydroxides released from the cement hydration which can facilitate the reactions of GGBS, associated with higher early-age strengths (Robins *et al.* 2006). This may make GGBS concrete a good application in China and other Asian countries which have the similar hot climatic conditions in summer. It should be noted that GGBS concretes under hot environment are more sensitive to a poor curing, i.e. insufficient moisture due to the high evaporation rate from fresh concrete (Al-Gahtani 2010). The strength and permeability of GGBS concrete was found to be seriously impaired when such a poor curing condition was provided.

Thermal stresses arising from cement hydration will cause thermal cracking if they exceed the tensile strength of the concrete. It is important to quantify these thermal stresses to ensure that the maximum crack width requirements are satisfied. Bamforth (2007) and Dhir *et al.* (2006) introduced a short-term temperature difference value  $T_1$  (°C) to define the difference between the peak temperature during cement hydration and the ambient temperature at the time of casting measured in different concrete mixes under different curing conditions. Furthermore, Bamforth (2007) introduced a restraint factor  $R$  to define the different restraints provided by the lateral resistance system (LRS), e.g. columns, shear walls and foundations. The introductions of  $T_1$  and  $R$  factors facilitate the calculations of thermal actions in long-span concrete. These factors, however, may not be entirely applicable to practical construction because they were often carried out without sufficiently consideration of the following construction and design practices:

- 1) The difference in the LRS of different geometric sizes, material properties and locations may not be sufficiently addressed by a constant  $R$  factor;
- 2) The construction sequence and its effect on thermal contraction in concrete;
- 3) The need to consider in-plane stresses in concrete slabs due to thermal contraction in



Fig. 1 A pour gap in a concrete beam

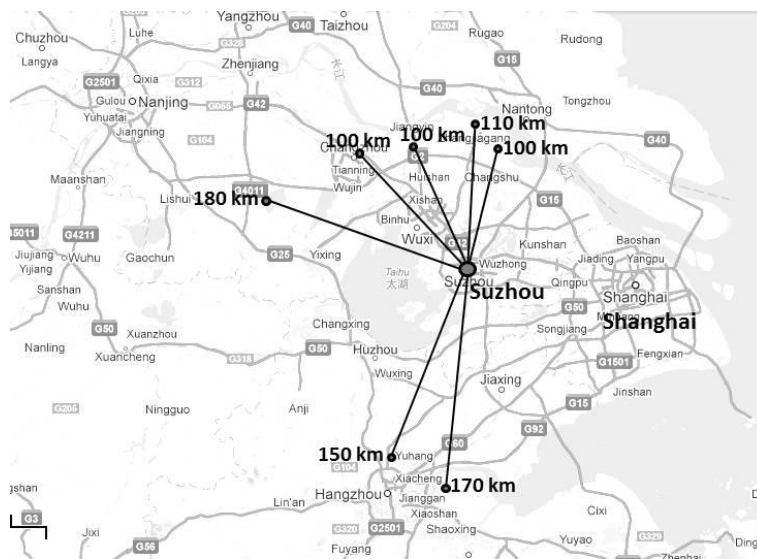


Fig. 2 Major steel companies in Jiangsu Province and their approximate distance (km) to Suzhou

conjunction with the out-of-plane stresses under permanent actions at the serviceability limit state when maximum crack widths are calculated.

GGBS is a high-volume and low-unit-value commodity. Its gate price is similar to that of CEM I cement in China. This makes the transportation cost a determining factor. A direct saving in GGBS used in low-grade blended cement can only be achieved if the construction site was located closer to the steel companies producing GGBS. This assumption does not seem to be applicable in many major cities in China (Tang *et al.* 2013). An example is given in Suzhou (Jiangsu Province, China), where XJTLU is located. More than 10% of nationwide steel is produced in Jiangsu

Province and the supply of GGBS should be ensured in comparison to most cities in China. Based on the market research, CEM I can be provided by local suppliers within a transportation distance no more than 10km. GGBS is however used within a distance of 100km radius from the source (Fig. 2). The long-distance delivery of GGBS not only elevates the cost, but also has a significant environmental impact, e.g. CO<sub>2</sub> emissions from vehicles. There is therefore no direct economic benefit from using GGBS to replace CEM I in concrete, except for its thermal advantages.

## 2. Objectives

It is a common assumption that GGBS concrete lacks sufficient strength at an early age and this might prevent its in-situ concrete applications. It is therefore useful to encourage the application of GGBS in long-span concrete structures by verifying that this detrimental effect on strength can be mitigated by the reduced thermal contraction. Another objective of this project is to encourage the use of GGBS in long-span concrete structures by minimising the use of more expensive crack control reinforcement, which could be a high value application in China. This is primarily achieved based on experimental work and finite element analysis (FEA) using Oasys GSA (2014). Oasys GSA is a general structural analysis program which has been used to model the effect of thermal actions on concrete elements (Tang *et al.* 2013). A case study has been conducted of a four-storey commercial office accommodation block, shown in Figs. 3-4. This office block is 75 m long and 37.5 m wide. C30/37 concrete flat slabs are used at all floor levels. These slabs span up to a maximum of 7.5 m, which provides a high flexibility for service penetrations and have been commonly adopted for commercial and office accommodations. Ground bearing slabs support slabs at the ground floor level. The structural frame is founded on piles. Additional parameters used in this model include:

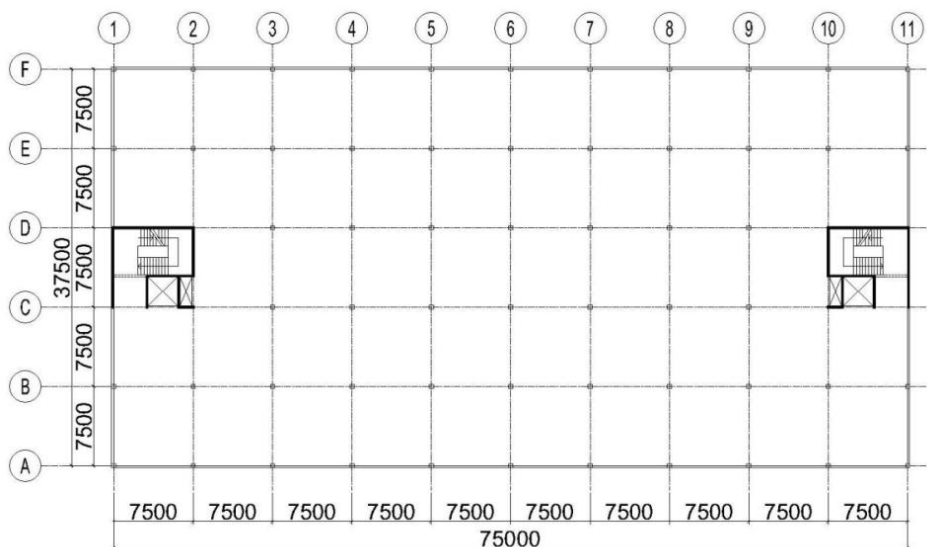


Fig. 3 Case study: Level 1 to Level 4 layout

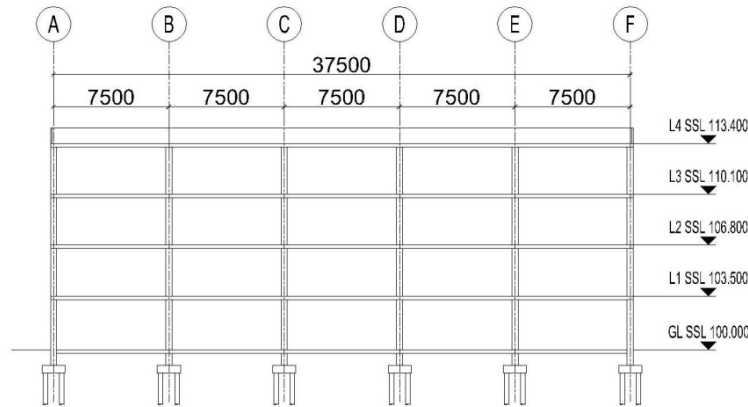


Fig. 4 Case study: Section through GL 3

- Concrete flat slabs, C30/37, 300 mm thick
- Concrete columns, C35/45, 400 mm×400 mm section
- Concrete shear/stairwell cores, C35/45, 200 mm thick

Thermal movements in slabs are restrained along the longitudinal direction by the concrete shear walls located between gridlines (GL) GL C-D: GL 1-2 and GL 10-11. Slabs were modelled using up to 70% CEM I replaced with GGBS to investigate the potential crack mitigation effects of GGBS. Results from a laboratory study (Section 3) were used as inputs for the FEA modelling (Section 6).

### 3. Concrete mixes and strength test

In this project, the following concrete mixes were developed to investigate the effect of partial replacement of CEM I with GGBS on the compressive strength of concrete:

- 0%GGBS, total binder content: 398 kg/m<sup>3</sup>
- 15%GGBS, total binder content: 398 kg/m<sup>3</sup>
- 30%GGBS, total binder content: 398 kg/m<sup>3</sup>
- 50%GGBS, total binder content: 438 kg/m<sup>3</sup>
- 70%GGBS, total binder content: 478 kg/m<sup>3</sup>

The target of all mixes was to develop C30/37 concrete with a suitable workability for floor slab casting. BS 8500-1 (2006) recommends a slump range between 100 mm and 150 mm for slab casting. A free water binder ratio (W/B) of approximately 0.50 was required for all mixes to achieve the same slump ratio of 100 mm. This might be attributed to the high specific surface value of GGBS particles, 425m<sup>2</sup>/kg, which was determined by the manufacturer. The total binder content was increased by 10% and 20% respectively in ‘50%GGBS’ and ‘70%GGBS’ mixes to maintain the early-age strength despite the replacement of CEM I cement with GGBS. Standard concrete cube specimens, 150 × 150 × 150 mm, were cast and cured at 20°C. Within 24 hours of casting, the

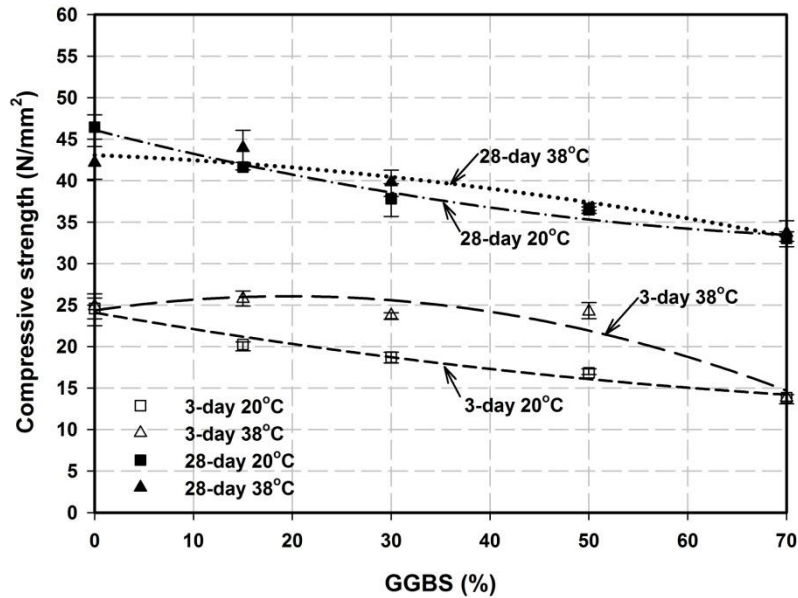


Fig. 5 3-day and 28-day GGBS concrete compressive strengths

cube specimens were demoulded and respectively placed into two water curing tanks which were set at 20°C and 38°C. The latter represents hot summer climatic conditions in Suzhou and Shanghai.

Partial replacement of CEM I with GGBS was observed to have a retarding effect on the early-age strength of concrete under the standard curing temperature regime of 20°C, as shown in Fig. 5. The 3-day compressive strengths of all GGBS concrete mixes were lower than that of CEM I concrete (0%GGBS). This detrimental effect however became less significant at a higher curing temperature of 38°C. The average 3-day compressive strength of '50%GGBS' was 24.0N/mm<sup>2</sup> which was almost same as the 3-day compressive strength of '0%GGBS', 24.9N/mm<sup>2</sup>. This indicates that high temperature curing has a beneficiary effect on the compressive strength of concrete at an early age and this finding agrees with Robins *et al.* (2006). The high curing temperature however was observed to have a detrimental effect on the 28-day compressive strength (Fig. 5). This detrimental effect nevertheless became less significant when part of CEM I was replaced with GGBS. This indicates the long-term strength of GGBS concrete was less adversely affected by high temperature curing compared to CEM I only mixes and this finding agrees with Barnett *et al.* (2006).

#### 4. Concrete semi-adiabatic calorimetry test

The curing conditions of long-span concrete slabs were simulated by concrete specimens cured semi-adiabatically to investigate the effect of GGBS on the peak hydration temperatures of concrete. Concrete slab specimens, 350 × 250 × 300 mm, were cast inside the insulated plywood

box (Fig. 6). Four sides of the specimen were insulated with 2 cm thick expanded polystyrene sheets to simulate the curing conditions of long-span concrete slabs. The bottom of the specimen was in contact with plywood formwork resting on top of the steel base of the environmental chamber. This allows the heat transfer through the plywood which is similar to the expected thermal conditions of suspended floor slabs cast upon the plywood formwork onsite. The environmental chamber temperature was set at 20°C or 38°C. The latter represents hot climatic conditions in Suzhou and Shanghai. Thermocouples, with an accuracy of  $\pm 0.1^\circ\text{C}$ , were placed in the centre of concrete and in the chamber to determine the difference between the peak temperature during the cement hydration reaction and the ambient temperature at the time of casting, i.e. T1 values. The following concrete mixes were developed to investigate the effect of partial replacement of CEM I with GGBS on the heat development in a suspended concrete slab. Their mix proportions were same as those used for strength tests in Section 3.

- 0% GGBS, total binder content:  $398 \text{ kg/m}^3$
- 50% GGBS, total binder content:  $438 \text{ kg/m}^3$
- 70% GGBS, total binder content:  $478 \text{ kg/m}^3$

As the GGBS content increases, the rate of hydration decreases at both 20°C and 38°C curing temperatures (Fig. 7 (a)-(b)). At 38°C curing temperature, the hydration rates (Fig. 7(b)) were observed to be much higher than that at 20°C (Fig. 7(a)). This indicates that a higher curing temperature accelerates the hydration of both CEM I and GGBS mixes and this finding agrees with Robins *et al.* (2006). As the GGBS content increases, T1 values decrease. This indicates a beneficiary thermal effect of using GGBS to replace CEM I. With up to 50% of CEM I replaced with GGBS, the thermal loading or the T1 values reduced from 12.5°C to 6.3°C at 38°C curing (Fig. 7 (b)). The actual temperature of the environmental chamber has been monitored and it was found to be generally within  $\pm 1^\circ\text{C}$  of the prescribed temperature, as shown in Fig. 8.

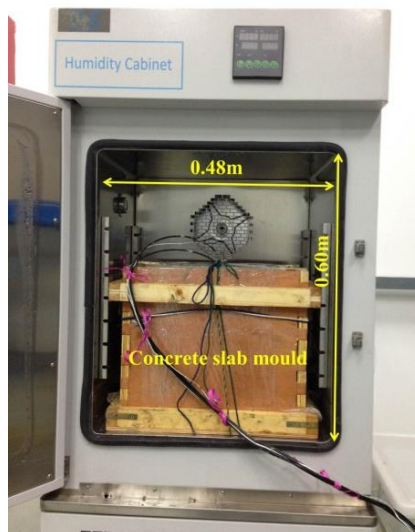


Fig. 6 Concrete slab mould inside the environmental chamber

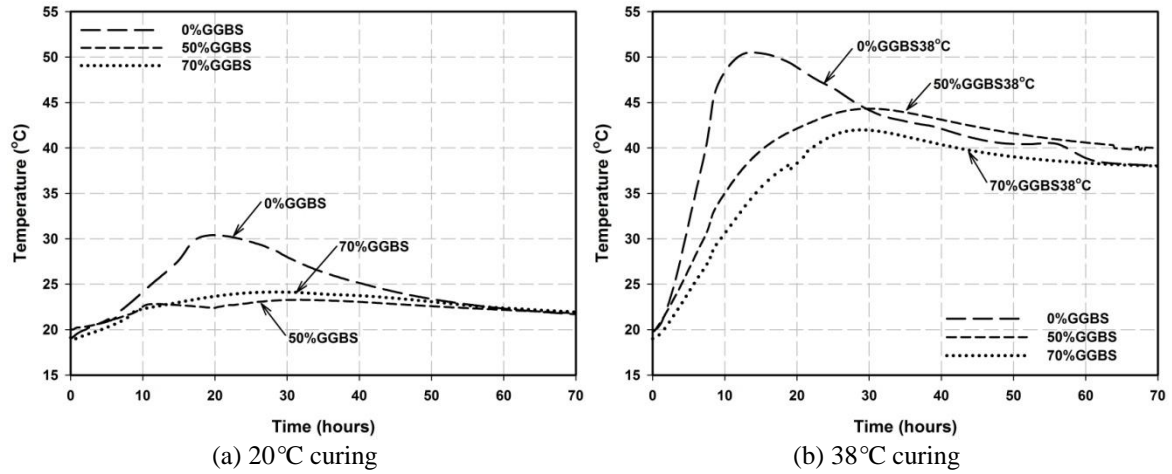


Fig. 7 Semi-adiabatic test result

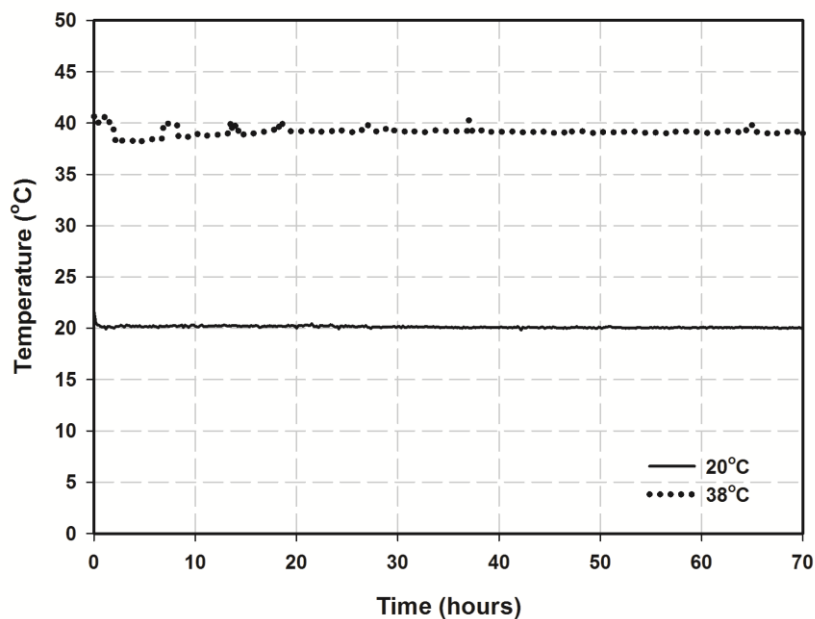


Fig. 8 Environmental chamber temperature variations (prescribed at 20°C and 38°C respectively)

## 5. Concrete autogenous shrinkage

Autogenous shrinkage is a short-term effect caused by the hydration of cement. Eurocode 2 (2004) gives Eq. (1) to estimate the autogenous shrinkage strain and this has been used in this project to calculate concrete early-age shrinkage.

Table 1 Autogenous shrinkage for C30/37 concrete

Time period(days)	$\varepsilon_{ca}$ ( $\times 10^{-6}$ )
3	14.6
28	32.6
100	43.2
365	48.9
Infinity	50.0

 Table 2  $\Delta T$  for C30/37 concrete

Time period (days)	$\Delta T_c$ ( $^{\circ}\text{C}$ )
3	1.5
28	3.3
100	4.3
365	4.9
Infinity	5.0

$$\varepsilon_{ca} = 2.5(f_{ck} - 10) \times [1 - \exp(-0.2 \times t^{0.5})] \times 10^{-6} \quad (1)$$

where:

$\varepsilon_{ca}$  : Autogenous shrinkage strain

$t$  : Age of concrete (days)

$f_{ck}$  : Characteristic compressive cylinder strength of concrete at 28 days ( $\text{N}/\text{mm}^2$ )

Autogenous shrinkage occurs over a longer duration than early-age thermal contraction although a large percentage takes place soon after casting, as shown in Table 1. Autogenous shrinkage has been converted to an equivalent temperature range,  $\Delta T$  ( $^{\circ}\text{C}$ ), according to Eq. (2).  $\Delta T$  was calculated by dividing the strains (Table 1) by the coefficient of thermal expansion,  $10 \times 10^{-6}/^{\circ}\text{C}$  (BSI 2004). Calculated results are shown in Table 2.

$$\Delta T = \varepsilon_{ca} \div \alpha_c \quad (2)$$

where:

$\alpha_c$  : Linear coefficient of concrete thermal expansions

From a comparison of T1 (Fig. 7) and  $\Delta T$  (Table 3) values, autogenous shrinkage is much less significant compared to the thermal contraction from cement hydration at an early age. The 3-day autogenic shrinkage is equivalent to a thermal contraction of  $1.5^{\circ}\text{C}$ . This is much less significant than the actual thermal contraction temperatures which occur in concrete without using GGBS, i.e.  $12.5^{\circ}\text{C}$ . Autogenous shrinkage has been incorporated into the thermal analysis in this project. The combined effect of T1 and  $\Delta T$  was used in the thermal analysis (Section 6) to define the early-age thermal actions. The presence of GGBS may have a beneficiary effect on a reduced autogenous shrinkage in concrete (Kim *et al.* 2011). Verification of this beneficiary effect is an area of ongoing research.

## 6. Thermal analysis

Accurate modelling of restraints from LRS is not easily achieved using hand calculations. This became possible based on the availability of finite element software, for example Oasys GSA (2014). Concrete slabs and shear walls were represented as 2D element mesh comprised of flat shells (Fig. 9). The 2D slab elements were modelled with the same thickness as the in-situ slabs, 300 mm. Cracking in concrete was modelled using an iterative analysis procedure (The Concrete Society 2008). The stiffness of highly stressed slab elements (i.e. where the maximum principal stress is greater than the tensile strength of concrete) was gradually reduced to enable the redistribution of residual thermal stresses after the development of concrete cracks. To quantify the mitigation of thermal stresses in concrete slabs using GGBS, three different comparison analyses have been carried out using the same structural model:

- Slabs with concrete made from ‘0%GGBS’ and using supplementary crack control reinforcement provided in areas where the maximum principal stress is greater than the tensile strength of concrete. T1 value has been considered in conjunction with  $\Delta T$  value;
- A repeat analysis using ‘50%GGBS’;
- A repeat analysis using ‘70%GGBS’.

The tensile strength of concrete ( $f_t$ ), which defines the failure criterion of concrete in the numerical modelling, was determined based on the empirical formula Eq. (3) between  $f_t$  and  $f_c$ , the compressive strength of concrete (Neville 2011). The calculated 3-day tensile strengths of GGBS concrete ( $f_t$ ) are summarized in Table 3.

$$f_t = 0.12f_c^{0.7} \quad (3)$$

Finite element analysis (FEA) results indicate that there is a high risk of the formation of tensile cracks on Level 1 slabs (Fig. 10(a)). Level 1 has the greatest lateral restraint stiffness provided by the cantilever shear cores. The maximum tensile stresses developed in a large region adjacent to the shear walls exceed the tensile strength of concrete,  $f_t$ . Slab reinforcement designed upon ultimate limit state combinations may yield in this highly stressed region and result in concrete cracks of excessive width. The magnitude of the concrete tensile stresses has been evaluated and supplementary crack control reinforcement was provided to prevent the yield of existing slab reinforcement, as shown in Fig. 10 and summarized in Table 4. Extra binder requirements for 50%GGBS and 70%GGBS mixes, in comparison with 0%GGBS, are shown in Table 4 too. Considering the gate price of CEM I and GGBS is approximately 5% of steel, the cost of extra binder for 50%GGBS concrete to maintain the early-age strength is equivalent to 1.7 tonne worth steel, which is even higher than the amount of supplementary reinforcement. There is therefore no

Table 3 3-day tensile and compressive strength of concrete (38°C curing)

	$f_c$ (N/mm <sup>2</sup> )	$f_t$ (N/mm <sup>2</sup> )
0%GGBS	24.87	1.14
50%GGBS	24.23	1.12
70%GGBS	13.84	0.76

Table 4 Supplementary reinforcement required on level 1 slab (38°C curing)

	Supplementary reinforcement (tonne)	Extra binder required (tonne)
0%GGBS	4.385	0
50%GGBS	1.350	34
70%GGBS	1.273	67

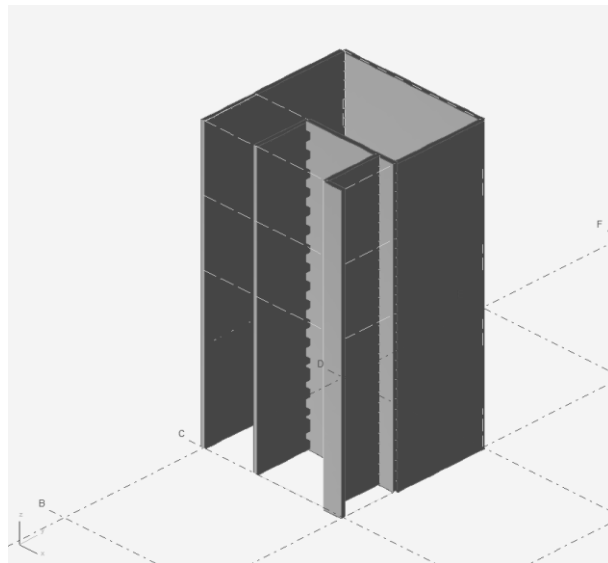
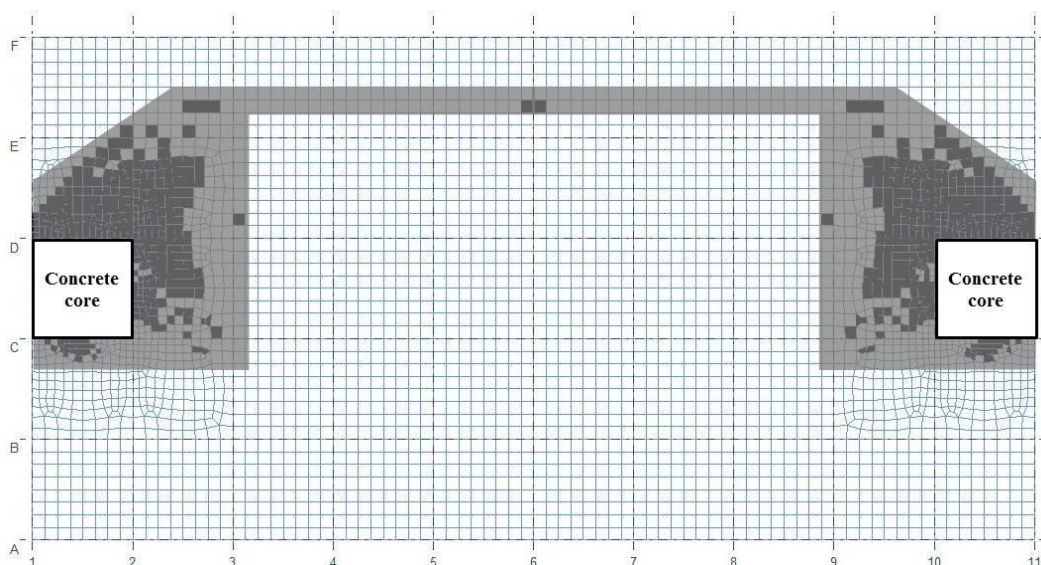
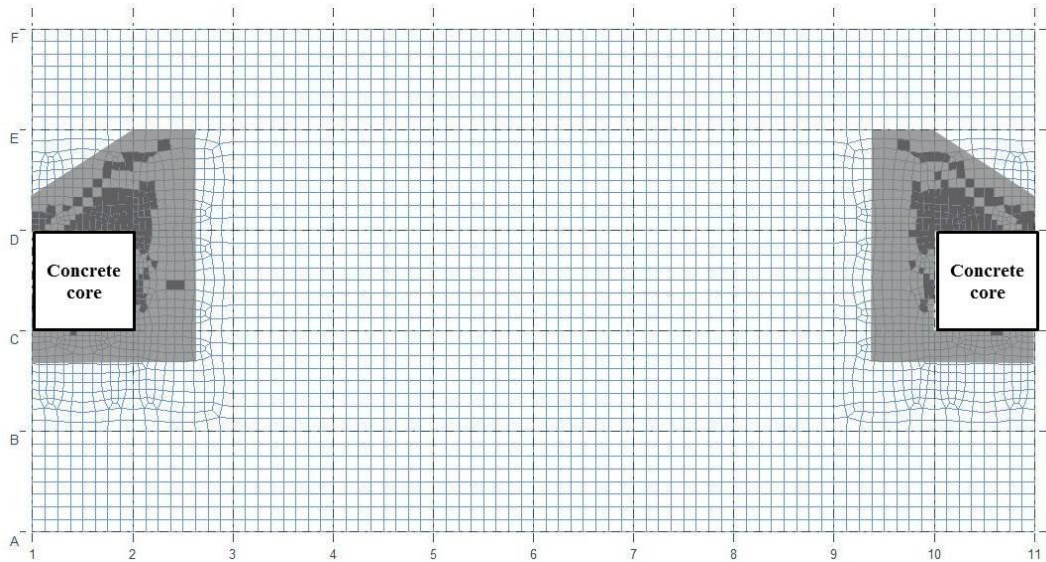


Fig. 9 Concrete core (shear wall) elements in GSA (isometric view)

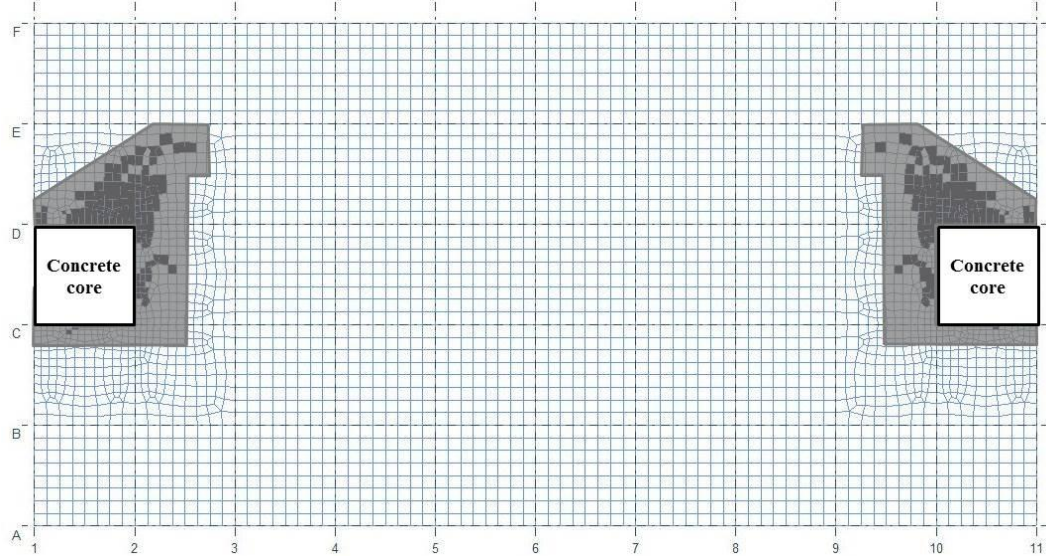


(a) Analysis 1: 0%GGBS – highly stressed elements  $> 1.14\text{N/mm}^2 (f_t)$  presented in shadow

Fig. 10 Highless stressed slab regions predicted by Oasys GSA modelling



(b) Analysis 2: 50%GGBS – highly stressed elements  $> 1.12\text{N/mm}^2 (f_t)$  presented in shadow



(c) Analysis 3: 70%GGBS – highly stressed elements  $> 0.76\text{N/mm}^2 (f_t)$  presented in shadow

Fig. 10 Continued

direct economic benefit to use GGBS to control thermal cracking in this case study. On the other hand, the use of recycled and reused materials represents an important strategy in the green building design, which in return will increase rental rates (Wang 2014). There is therefore scope to extend this study to calculate the whole-life cost of GGBS. This finding may be transferable to other Asian countries with similar summer climates and economic conditions.

The amount of supplementary reinforcement,  $A_s$ , was determined according to Eq. (4). In this project, 500MPa characteristic strength steel reinforcement is used to resist thermal actions in

slabs. Reinforcement anchorage length has not been considered in this modelling and it will require an additional cost.

$$A_s = \frac{\sigma \times d \times 1000}{f_y} \quad (4)$$

where:

$A_s$ : Supplementary reinforcement ( $\text{mm}^2$  per meter wide slab)

$\sigma$ : Maximum tensile stress in slabs (MPa)

$d$ : Slab thickness (mm), 300 mm in this case study

$f_y$ : Yield strength of supplementary reinforcement

The presence of GGBS effectively reduced thermal stresses at 38°C curing, and as a result the amount of supplementary crack control reinforcement required. With up to 50% of the cement replaced by GGBS, 69% of the total supplementary thermal crack control reinforcement can be saved in Level 1 slabs (Fig. 10(b)). It was observed that only 71% of supplementary crack control reinforcement could be saved when the replacement ratio was increased to 70% (Fig. 10(c)). This modest increase in saving can be attributed to the low early-age tensile strength of GGBS concrete, i.e. 0.76N/mm<sup>2</sup>.

## 7. Conclusions

The heat development from cement hydration can cause concrete early-age thermal contraction which accounts for the major part of the total early-age contraction in reinforced concrete elements. This influence is particularly significant in China and other Asian countries with hot summer climates. FEA based on Oasys GSA can be used to predict early-age thermal contraction and resulting stresses in concrete structural elements for design purposes. The effects of temperature variations and of time-dependent concrete volume change, including drying shrinkage, have been investigated in this project via a case study based investigation. The use of GGBS in concrete slabs can reduce the requirement for more expensive crack control reinforcement. With up to 50% of cement replaced by GGBS, nearly 70% of the supplementary crack control reinforcement can be saved. There is however no direct economic benefit due to the increased binder content in GGBS concrete to maintain the strength of concrete at early ages.

## References

- Al-Gahtani, A.S. (2010), "Effect of curing methods on the properties of plain and blended cement concretes", *Constr. Build. Mater.*, **24** (3), 308-14.
- Azenha, M., Faria, R. and Ferreira, D. (2009), "Identification of early-age concrete temperatures and strains: monitoring and numerical simulation", *Cement Concrete Compos.*, **31** (6), 369-378.
- Bamforth, P.B. (2007), *CIRIA C660 Early-age Thermal Crack Control in Concrete*, CIRIA, London, UK.
- Barnett, S.J., Soutsos, M.N., Millard, S.G. and Bungey, J.H. (2006), "Strength development of mortars containing ground granulated blast-furnace slag: Effect of curing temperature and determination of apparent activation energies", *Cement Concrete Res.*, **36** (3), 434-40.
- BSI (2004), *BS EN 1992-1-1: 2004 Design of Concrete Structures*, British Standards Institution (BSI), London, UK.

- BSI (2006), *BS 8500-1: 2006 Complementary British Standard to BS EN 206-1, Method of Specifying and Guidance for the Specifier*, British Standards Institution (BSI), London, UK.
- Da Silva, W.R.L., Milauer, V. and Temberk, P. (2013), "Upscaling semi-adiabatic measurements for simulating temperature evolution of mass concrete structures", *Mater. Struct.*, **2013**: 1-11.
- Dhir, R.K., Paine, K.A. and Zheng, L. (2006), *Design Data for Use Where Low Heat Cements are Used DTI Research Contract No. 39/680, CC2257*. Report No CTU 2704, University of Dundee, UK.
- Kim, G.Y., Lee, E.B., Nam, J.S. and Koo, K.M. (2011), "Analysis of hydration heat and autogenous shrinkage of high-strength mass concrete", *Mag. Concrete Res.*, **63** (5), 377-389.
- Lawrence, A.M., Tia, M., Ferraro, C.C. and Bergin, M. (2012), "Effect of early age strength on cracking in mass concrete containing different supplementary cementitious materials: experimental and finite-element investigation", *J. Mater. Civil Eng.*, **24** (4), 362-372.
- Neville, A.M. (2011), *Properties Concrete*. England, Pearson, London, UK.
- Oasys (2014), Oasys GSA 8.7, Oasys Limited.
- PRC Ministry of Construction (2002), *Code for Design of Concrete Structures*, PRC Ministry of Construction, Beijing, China.
- PRC Ministry of Construction (2008), *GB/T 18046-2008 Ground Granulated Blast Furnace Slag Used for Cement Concrete*, PRC Ministry of Construction, Beijing, China.
- Regourd, M. (1983), "Microanalytical studies (X-Ray Photo Electron Spectrometry) of surface hydration reactions of cement compounds", *Technology in the 1990s: Developments in Hydraulic Cements, Proceedings of a Royal Society Discussion Meeting*, London, UK.
- Robins, P.J., Austin, S.A. and Issaad, A. (2006), "Suitability of GGBFS as a cement replacement for concrete in hot arid climates", *Mater. Struct.*, **25** (10), 598-612.
- Tang, K. (2014), "High value applications of GGBS in China", *The 2014 World Congress on Advances in Civil, Environmental & Materials Research (ACEM14)*, Busan, Korea.
- Tang, K., Millard, S.G. and Beattie, G. (2013), "Technical and economic aspects of using GGBFS for crack control mitigation in long span reinforced concrete structures", *Constr. Build. Mater.*, **39** (1), 65-70.
- The Concrete Society (2008), *Technical Report No. 67 Movement, restraint and cracking in concrete structures*, The Concrete Society.
- Wang, W. (2014), "Why build green?", NetEase, Beijing, China. See <http://discover.news.163.com/special/whybuildgreen/> (accessed 11/12/2014).